

Search for $b \rightarrow u$ transitions in $B^- \rightarrow [K^+ \pi^- \pi^0]_D K^-$

B. Aubert,¹ M. Bona,¹ D. Boutigny,¹ Y. Karyotakis,¹ J. P. Lees,¹ V. Poireau,¹ X. Prudent,¹ V. Tisserand,¹ A. Zghiche,¹ J. Garra Tico,² E. Grauges,² L. Lopez,³ A. Palano,³ G. Eigen,⁴ B. Stugu,⁴ L. Sun,⁴ G. S. Abrams,⁵ M. Battaglia,⁵ D. N. Brown,⁵ J. Button-Shafer,⁵ R. N. Cahn,⁵ Y. Groyzman,⁵ R. G. Jacobsen,⁵ J. A. Kadyk,⁵ L. T. Kerth,⁵ Yu. G. Kolomensky,⁵ G. Kukartsev,⁵ D. Lopes Pegna,⁵ G. Lynch,⁵ L. M. Mir,⁵ T. J. Orimoto,⁵ M. T. Ronan,^{5,*} K. Tackmann,⁵ W. A. Wenzel,⁵ P. del Amo Sanchez,⁶ C. M. Hawkes,⁶ A. T. Watson,⁶ T. Held,⁷ H. Koch,⁷ B. Lewandowski,⁷ M. Pelizaeus,⁷ T. Schroeder,⁷ M. Steinke,⁷ D. Walker,⁸ D. J. Asgeirsson,⁹ T. Cuhadar-Donszelmann,⁹ B. G. Fulsom,⁹ C. Hearty,⁹ T. S. Mattison,⁹ J. A. McKenna,⁹ A. Khan,¹⁰ M. Saleem,¹⁰ L. Teodorescu,¹⁰ V. E. Blinov,¹¹ A. D. Bukin,¹¹ V. P. Druzhinin,¹¹ V. B. Golubev,¹¹ A. P. Onuchin,¹¹ S. I. Serebnyakov,¹¹ Yu. I. Skovpen,¹¹ E. P. Solodov,¹¹ K. Yu. Todyshev,¹¹ M. Bondioli,¹² S. Curry,¹² I. Eschrich,¹² D. Kirkby,¹² A. J. Lankford,¹² P. Lund,¹² M. Mandelkern,¹² E. C. Martin,¹² D. P. Stoker,¹² S. Abachi,¹³ C. Buchanan,¹³ S. D. Foulkes,¹⁴ J. W. Gary,¹⁴ F. Liu,¹⁴ O. Long,¹⁴ B. C. Shen,¹⁴ L. Zhang,¹⁴ H. P. Paar,¹⁵ S. Rahatlou,¹⁵ V. Sharma,¹⁵ J. W. Berryhill,¹⁶ C. Campagnari,¹⁶ A. Cunha,¹⁶ B. Dahmes,¹⁶ T. M. Hong,¹⁶ D. Kovalskyi,¹⁶ J. D. Richman,¹⁶ T. W. Beck,¹⁷ A. M. Eisner,¹⁷ C. J. Flacco,¹⁷ C. A. Heusch,¹⁷ J. Kroseberg,¹⁷ W. S. Lockman,¹⁷ T. Schalk,¹⁷ B. A. Schumm,¹⁷ A. Seiden,¹⁷ M. G. Wilson,¹⁷ L. O. Winstrom,¹⁷ E. Chen,¹⁸ C. H. Cheng,¹⁸ F. Fang,¹⁸ D. G. Hitlin,¹⁸ I. Narsky,¹⁸ T. Piatenko,¹⁸ F. C. Porter,¹⁸ R. Andreassen,¹⁹ G. Mancinelli,¹⁹ B. T. Meadows,¹⁹ K. Mishra,¹⁹ M. D. Sokoloff,¹⁹ F. Blanc,²⁰ P. C. Bloom,²⁰ S. Chen,²⁰ W. T. Ford,²⁰ J. F. Hirschauer,²⁰ A. Kreisel,²⁰ M. Nagel,²⁰ U. Nauenberg,²⁰ A. Olivas,²⁰ J. G. Smith,²⁰ K. A. Ulmer,²⁰ S. R. Wagner,²⁰ J. Zhang,²⁰ A. M. Gabareen,²¹ A. Soffer,²¹ W. H. Toki,²¹ R. J. Wilson,²¹ F. Winklmeier,²¹ D. D. Altenburg,²² E. Feltresi,²² A. Hauke,²² H. Jasper,²² J. Merkel,²² A. Petzold,²² B. Spaan,²² K. Wacker,²² V. Klose,²³ M. J. Kobel,²³ H. M. Lacker,²³ W. F. Mader,²³ R. Nogowski,²³ J. Schubert,²³ K. R. Schubert,²³ R. Schwierz,²³ J. E. Sundermann,²³ A. Volk,²³ D. Bernard,²⁴ G. R. Bonneaud,²⁴ E. Latour,²⁴ V. Lombardo,²⁴ Ch. Thiebaut,²⁴ M. Verderi,²⁴ P. J. Clark,²⁵ W. Gradl,²⁵ F. Muheim,²⁵ S. Playfer,²⁵ A. I. Robertson,²⁵ Y. Xie,²⁵ M. Andreotti,²⁶ D. Bettoni,²⁶ C. Bozzi,²⁶ R. Calabrese,²⁶ A. Cecchi,²⁶ G. Cibinetto,²⁶ P. Franchini,²⁶ E. Luppi,²⁶ M. Negrini,²⁶ A. Petrella,²⁶ L. Piemontese,²⁶ E. Prencipe,²⁶ V. Santoro,²⁶ F. Anulli,²⁷ R. Baldini-Ferrolli,²⁷ A. Calcaterra,²⁷ R. de Sangro,²⁷ G. Finocchiaro,²⁷ S. Pacetti,²⁷ P. Patteri,²⁷ I. M. Peruzzi,^{27,†} M. Piccolo,²⁷ M. Rama,²⁷ A. Zallo,²⁷ A. Buzzo,²⁸ R. Contri,²⁸ M. Lo Vetere,²⁸ M. M. Macri,²⁸ M. R. Monge,²⁸ S. Passaggio,²⁸ C. Patrignani,²⁸ E. Robutti,²⁸ A. Santroni,²⁸ S. Tosi,²⁸ K. S. Chaisanguanthum,²⁹ M. Morii,²⁹ J. Wu,²⁹ R. S. Dubitzky,³⁰ J. Marks,³⁰ S. Schenk,³⁰ U. Uwer,³⁰ D. J. Bard,³¹ P. D. Dauncey,³¹ R. L. Flack,³¹ J. A. Nash,³¹ W. Panduro Vazquez,³¹ M. Tibbetts,³¹ P. K. Behera,³² X. Chai,³² M. J. Charles,³² U. Mallik,³² V. Ziegler,³² J. Cochran,³³ H. B. Crawley,³³ L. Dong,³³ V. Eyges,³³ W. T. Meyer,³³ S. Prell,³³ E. I. Rosenberg,³³ A. E. Rubin,³³ Y. Y. Gao,³⁴ A. V. Gritsan,³⁴ Z. J. Guo,³⁴ C. K. Lae,³⁴ A. G. Denig,³⁵ M. Fritsch,³⁵ G. Schott,³⁵ N. Arnaud,³⁶ J. Béquilleux,³⁶ M. Davier,³⁶ G. Grosdidier,³⁶ A. Höcker,³⁶ V. Lepeltier,³⁶ F. Le Diberder,³⁶ A. M. Lutz,³⁶ S. Pruvot,³⁶ S. Rodier,³⁶ P. Roudeau,³⁶ M. H. Schune,³⁶ J. Serrano,³⁶ V. Sordini,³⁶ A. Stocchi,³⁶ W. F. Wang,³⁶ G. Wormser,³⁶ D. J. Lange,³⁷ D. M. Wright,³⁷ I. Bingham,³⁸ C. A. Chavez,³⁸ I. J. Forster,³⁸ J. R. Fry,³⁸ E. Gabathuler,³⁸ R. Gamet,³⁸ D. E. Hutchcroft,³⁸ D. J. Payne,³⁸ K. C. Schofield,³⁸ C. Touramanis,³⁸ A. J. Bevan,³⁹ K. A. George,³⁹ F. Di Lodovico,³⁹ W. Menges,³⁹ R. Sacco,³⁹ G. Cowan,⁴⁰ H. U. Flaecher,⁴⁰ D. A. Hopkins,⁴⁰ S. Paramesvaran,⁴⁰ F. Salvatore,⁴⁰ A. C. Wren,⁴⁰ D. N. Brown,⁴¹ C. L. Davis,⁴¹ J. Allison,⁴² N. R. Barlow,⁴² R. J. Barlow,⁴² Y. M. Chia,⁴² C. L. Edgar,⁴² G. D. Lafferty,⁴² T. J. West,⁴² J. I. Yi,⁴² J. Anderson,⁴³ C. Chen,⁴³ A. Jawahery,⁴³ D. A. Roberts,⁴³ G. Simi,⁴³ J. M. Tuggle,⁴³ G. Blaylock,⁴⁴ C. Dallapiccola,⁴⁴ S. S. Hertzbach,⁴⁴ X. Li,⁴⁴ T. B. Moore,⁴⁴ E. Salvati,⁴⁴ S. Saremi,⁴⁴ R. Cowan,⁴⁵ D. Dujmic,⁴⁵ P. H. Fisher,⁴⁵ K. Koeneke,⁴⁵ G. Sciolla,⁴⁵ S. J. Sekula,⁴⁵ M. Spitznagel,⁴⁵ F. Taylor,⁴⁵ R. K. Yamamoto,⁴⁵ M. Zhao,⁴⁵ Y. Zheng,⁴⁵ S. E. Mclachlin,^{46,*} P. M. Patel,⁴⁶ S. H. Robertson,⁴⁶ A. Lazzaro,⁴⁷ F. Palombo,⁴⁷ J. M. Bauer,⁴⁸ L. Cremaldi,⁴⁸ V. Eschenburg,⁴⁸ R. Godang,⁴⁸ R. Kroeger,⁴⁸ D. A. Sanders,⁴⁸ D. J. Summers,⁴⁸ H. W. Zhao,⁴⁸ S. Brunet,⁴⁹ D. Côté,⁴⁹ M. Simard,⁴⁹ P. Taras,⁴⁹ F. B. Viaud,⁴⁹ H. Nicholson,⁵⁰ G. De Nardo,⁵¹ F. Fabozzi,^{51,‡} L. Lista,⁵¹ D. Monorchio,⁵¹ C. Sciacca,⁵¹ M. A. Baak,⁵² G. Raven,⁵² H. L. Snoek,⁵² C. P. Jessop,⁵³ J. M. LoSecco,⁵³ G. Benelli,⁵⁴ L. A. Corwin,⁵⁴ K. Honscheid,⁵⁴ H. Kagan,⁵⁴ R. Kass,⁵⁴ J. P. Morris,⁵⁴ A. M. Rahimi,⁵⁴ J. J. Regensburger,⁵⁴ Q. K. Wong,⁵⁴ N. L. Blount,⁵⁵ J. Brau,⁵⁵ R. Frey,⁵⁵ O. Igonkina,⁵⁵ J. A. Kolb,⁵⁵ M. Lu,⁵⁵ R. Rahmat,⁵⁵ N. B. Sinev,⁵⁵ D. Strom,⁵⁵ J. Strube,⁵⁵ E. Torrence,⁵⁵ N. Gagliardi,⁵⁶ A. Gaz,⁵⁶ M. Margoni,⁵⁶ M. Morandin,⁵⁶ A. Pompili,⁵⁶ M. Posocco,⁵⁶ M. Rotondo,⁵⁶ F. Simonetto,⁵⁶ R. Stroili,⁵⁶ C. Voci,⁵⁶ E. Ben-Haim,⁵⁷ H. Briand,⁵⁷ G. Calderini,⁵⁷ J. Chauveau,⁵⁷ P. David,⁵⁷ L. Del Buono,⁵⁷ Ch. de la Vaissière,⁵⁷ O. Hamon,⁵⁷ Ph. Leruste,⁵⁷ J. Malcès,⁵⁷ J. Ocariz,⁵⁷ A. Perez,⁵⁷ L. Gladney,⁵⁸ M. Biasini,⁵⁹ R. Covarelli,⁵⁹ E. Manoni,⁵⁹ C. Angelini,⁶⁰ G. Batignani,⁶⁰ S. Bettarini,⁶⁰ M. Carpinelli,⁶⁰ R. Cenci,⁶⁰ A. Cervelli,⁶⁰ F. Forti,⁶⁰ M. A. Giorgi,⁶⁰ A. Lusiani,⁶⁰ G. Marchiori,⁶⁰ M. A. Mazur,⁶⁰ M. Morganti,⁶⁰ N. Neri,⁶⁰

E. Paoloni,⁶⁰ G. Rizzo,⁶⁰ J. J. Walsh,⁶⁰ M. Haire,⁶¹ J. Biesiada,⁶² P. Elmer,⁶² Y. P. Lau,⁶² C. Lu,⁶² J. Olsen,⁶² A. J. S. Smith,⁶² A. V. Telnov,⁶² E. Baracchini,⁶³ F. Bellini,⁶³ G. Cavoto,⁶³ A. D’Orazio,⁶³ D. del Re,⁶³ E. Di Marco,⁶³ R. Faccini,⁶³ F. Ferrarotto,⁶³ F. Ferroni,⁶³ M. Gaspero,⁶³ P. D. Jackson,⁶³ L. Li Gioi,⁶³ M. A. Mazzoni,⁶³ S. Morganti,⁶³ G. Piredda,⁶³ F. Polci,⁶³ F. Renga,⁶³ C. Voena,⁶³ M. Ebert,⁶⁴ T. Hartmann,⁶⁴ H. Schröder,⁶⁴ R. Waldi,⁶⁴ T. Adye,⁶⁵ G. Castelli,⁶⁵ B. Franek,⁶⁵ E. O. Olaiya,⁶⁵ S. Ricciardi,⁶⁵ W. Roethel,⁶⁵ F. F. Wilson,⁶⁵ R. Aleksan,⁶⁶ S. Emery,⁶⁶ M. Escalier,⁶⁶ A. Gaidot,⁶⁶ S. F. Ganzhur,⁶⁶ G. Hamel de Monchenault,⁶⁶ W. Kozanecki,⁶⁶ G. Vasseur,⁶⁶ Ch. Yèche,⁶⁶ M. Zito,⁶⁶ X. R. Chen,⁶⁷ H. Liu,⁶⁷ W. Park,⁶⁷ M. V. Purohit,⁶⁷ J. R. Wilson,⁶⁷ M. T. Allen,⁶⁸ D. Aston,⁶⁸ R. Bartoldus,⁶⁸ P. Bechtle,⁶⁸ N. Berger,⁶⁸ R. Claus,⁶⁸ J. P. Coleman,⁶⁸ M. R. Convery,⁶⁸ J. C. Dingfelder,⁶⁸ J. Dorfan,⁶⁸ G. P. Dubois-Felsmann,⁶⁸ W. Dunwoodie,⁶⁸ R. C. Field,⁶⁸ T. Glanzman,⁶⁸ S. J. Gowdy,⁶⁸ M. T. Graham,⁶⁸ P. Grenier,⁶⁸ C. Hast,⁶⁸ T. Hryn’ova,⁶⁸ W. R. Innes,⁶⁸ J. Kaminski,⁶⁸ M. H. Kelsey,⁶⁸ H. Kim,⁶⁸ P. Kim,⁶⁸ M. L. Kocian,⁶⁸ D. W. G. S. Leith,⁶⁸ S. Li,⁶⁸ S. Luitz,⁶⁸ V. Luth,⁶⁸ H. L. Lynch,⁶⁸ D. B. MacFarlane,⁶⁸ H. Marsiske,⁶⁸ R. Messner,⁶⁸ D. R. Muller,⁶⁸ C. P. O’Grady,⁶⁸ I. Ofte,⁶⁸ A. Perazzo,⁶⁸ M. Perl,⁶⁸ T. Pulliam,⁶⁸ B. N. Ratcliff,⁶⁸ A. Roodman,⁶⁸ A. A. Salnikov,⁶⁸ R. H. Schindler,⁶⁸ J. Schwiening,⁶⁸ A. Snyder,⁶⁸ J. Stelzer,⁶⁸ D. Su,⁶⁸ M. K. Sullivan,⁶⁸ K. Suzuki,⁶⁸ S. K. Swain,⁶⁸ J. M. Thompson,⁶⁸ J. Va’vra,⁶⁸ N. van Bakel,⁶⁸ A. P. Wagner,⁶⁸ M. Weaver,⁶⁸ W. J. Wisniewski,⁶⁸ M. Wittgen,⁶⁸ D. H. Wright,⁶⁸ A. K. Yarritu,⁶⁸ K. Yi,⁶⁸ C. C. Young,⁶⁸ P. R. Burchat,⁶⁹ A. J. Edwards,⁶⁹ S. A. Majewski,⁶⁹ B. A. Petersen,⁶⁹ L. Wilden,⁶⁹ S. Ahmed,⁷⁰ M. S. Alam,⁷⁰ R. Bula,⁷⁰ J. A. Ernst,⁷⁰ V. Jain,⁷⁰ B. Pan,⁷⁰ M. A. Saeed,⁷⁰ F. R. Wappler,⁷⁰ S. B. Zain,⁷⁰ W. Bugg,⁷¹ M. Krishnamurthy,⁷¹ S. M. Spanier,⁷¹ R. Eckmann,⁷² J. L. Ritchie,⁷² A. M. Ruland,⁷² C. J. Schilling,⁷² R. F. Schwitters,⁷² J. M. Izen,⁷³ X. C. Lou,⁷³ S. Ye,⁷³ F. Bianchi,⁷⁴ F. Gallo,⁷⁴ D. Gamba,⁷⁴ M. Pelliccioni,⁷⁴ M. Bomben,⁷⁵ L. Bosisio,⁷⁵ C. Cartaro,⁷⁵ F. Cossutti,⁷⁵ G. Della Ricca,⁷⁵ L. Lanceri,⁷⁵ L. Vitale,⁷⁵ V. Azzolini,⁷⁶ N. Lopez-March,⁷⁶ F. Martinez-Vidal,^{76,8} D. A. Milanes,⁷⁶ A. Oyanguren,⁷⁶ J. Albert,⁷⁷ Sw. Banerjee,⁷⁷ B. Bhuyan,⁷⁷ K. Hamano,⁷⁷ R. Kowalewski,⁷⁷ I. M. Nugent,⁷⁷ J. M. Roney,⁷⁷ R. J. Sobie,⁷⁷ P. F. Harrison,⁷⁸ J. Ilic,⁷⁸ T. E. Latham,⁷⁸ G. B. Mohanty,⁷⁸ M. Pappagallo,^{78,11} H. R. Band,⁷⁹ X. Chen,⁷⁹ S. Dasu,⁷⁹ K. T. Flood,⁷⁹ J. J. Hollar,⁷⁹ P. E. Kutter,⁷⁹ Y. Pan,⁷⁹ M. Pierini,⁷⁹ R. Prepost,⁷⁹ S. L. Wu,⁷⁹ and H. Neal⁸⁰

(The *BABAR* Collaboration)

¹Laboratoire de Physique des Particules, IN2P3/CNRS et Université de Savoie, F-74941 Annecy-Le-Vieux, France

²Universitat de Barcelona, Facultat de Física, Departament ECM, E-08028 Barcelona, Spain

³Dipartimento di Fisica and INFN, Università di Bari, I-70126 Bari, Italy

⁴University of Bergen, Institute of Physics, N-5007 Bergen, Norway

⁵Lawrence Berkeley National Laboratory, Berkeley, California 94720, USA
and University of California, Berkeley, California 94720, USA

⁶University of Birmingham, Birmingham, B15 2TT, United Kingdom

⁷Ruhr Universität Bochum, Institut für Experimentalphysik I, D-44780 Bochum, Germany

⁸University of Bristol, Bristol BS8 1TL, United Kingdom

⁹University of British Columbia, Vancouver, British Columbia, Canada V6T 1Z1

¹⁰Brunel University, Uxbridge, Middlesex UB8 3PH, United Kingdom

¹¹Budker Institute of Nuclear Physics, Novosibirsk 630090, Russia

¹²University of California at Irvine, Irvine, California 92697, USA

¹³University of California at Los Angeles, Los Angeles, California 90024, USA

¹⁴University of California at Riverside, Riverside, California 92521, USA

¹⁵University of California at San Diego, La Jolla, California 92093, USA

¹⁶University of California at Santa Barbara, Santa Barbara, California 93106, USA

¹⁷University of California at Santa Cruz, Institute for Particle Physics, Santa Cruz, California 95064, USA

¹⁸California Institute of Technology, Pasadena, California 91125, USA

¹⁹University of Cincinnati, Cincinnati, Ohio 45221, USA

²⁰University of Colorado, Boulder, Colorado 80309, USA

²¹Colorado State University, Fort Collins, Colorado 80523, USA

²²Universität Dortmund, Institut für Physik, D-44221 Dortmund, Germany

²³Technische Universität Dresden, Institut für Kern- und Teilchenphysik, D-01062 Dresden, Germany

²⁴Laboratoire Leprince-Ringuet, CNRS/IN2P3, Ecole Polytechnique, F-91128 Palaiseau, France

²⁵University of Edinburgh, Edinburgh EH9 3JZ, United Kingdom

²⁶Dipartimento di Fisica and INFN, Università di Ferrara, I-44100 Ferrara, Italy

²⁷Laboratori Nazionali di Frascati dell’INFN, I-00044 Frascati, Italy

²⁸Dipartimento di Fisica and INFN, Università di Genova, I-16146 Genova, Italy

²⁹Harvard University, Cambridge, Massachusetts 02138, USA

- ³⁰Universität Heidelberg, Physikalisches Institut, Philosophenweg 12, D-69120 Heidelberg, Germany
- ³¹Imperial College London, London, SW7 2AZ, United Kingdom
- ³²University of Iowa, Iowa City, Iowa 52242, USA
- ³³Iowa State University, Ames, Iowa 50011-3160, USA
- ³⁴Johns Hopkins University, Baltimore, Maryland 21218, USA
- ³⁵Universität Karlsruhe, Institut für Experimentelle Kernphysik, D-76021 Karlsruhe, Germany
- ³⁶Laboratoire de l'Accélérateur Linéaire, IN2P3/CNRS et Université Paris-Sud 11, Centre Scientifique d'Orsay, B. P. 34, F-91898 ORSAY Cedex, France
- ³⁷Lawrence Livermore National Laboratory, Livermore, California 94550, USA
- ³⁸University of Liverpool, Liverpool L69 7ZE, United Kingdom
- ³⁹Queen Mary, University of London, E1 4NS, United Kingdom
- ⁴⁰University of London, Royal Holloway, Surrey TW20 0EX, United Kingdom and Bedford New College, Egham, Surrey TW20 0EX, United Kingdom
- ⁴¹University of Louisville, Louisville, Kentucky 40292, USA
- ⁴²University of Manchester, Manchester M13 9PL, United Kingdom
- ⁴³University of Maryland, College Park, Maryland 20742, USA
- ⁴⁴University of Massachusetts, Amherst, Massachusetts 01003, USA
- ⁴⁵Massachusetts Institute of Technology, Laboratory for Nuclear Science, Cambridge, Massachusetts 02139, USA
- ⁴⁶McGill University, Montréal, Québec, Canada H3A 2T8
- ⁴⁷Dipartimento di Fisica and INFN, Università di Milano, I-20133 Milano, Italy
- ⁴⁸University of Mississippi, University, Mississippi 38677, USA
- ⁴⁹Université de Montréal, Physique des Particules, Montréal, Québec, Canada H3C 3J7
- ⁵⁰Mount Holyoke College, South Hadley, Massachusetts 01075, USA
- ⁵¹Dipartimento di Scienze Fisiche and INFN, Università di Napoli Federico II, I-80126, Napoli, Italy
- ⁵²NIKHEF, National Institute for Nuclear Physics and High Energy Physics, NL-1009 DB Amsterdam, The Netherlands
- ⁵³University of Notre Dame, Notre Dame, Indiana 46556, USA
- ⁵⁴Ohio State University, Columbus, Ohio 43210, USA
- ⁵⁵University of Oregon, Eugene, Oregon 97403, USA
- ⁵⁶Dipartimento di Fisica and INFN, Università di Padova, I-35131 Padova, Italy
- ⁵⁷Laboratoire de Physique Nucléaire et de Hautes Energies, IN2P3/CNRS, Université Pierre et Marie Curie-Paris6, Université Denis Diderot-Paris7, F-75252 Paris, France
- ⁵⁸University of Pennsylvania, Philadelphia, Pennsylvania 19104, USA
- ⁵⁹Dipartimento di Fisica and INFN, Università di Perugia, I-06100 Perugia, Italy
- ⁶⁰Dipartimento di Fisica, Università di Pisa, Scuola Normale Superiore and INFN, I-56127 Pisa, Italy
- ⁶¹Prairie View A&M University, Prairie View, Texas 77446, USA
- ⁶²Princeton University, Princeton, New Jersey 08544, USA
- ⁶³Dipartimento di Fisica and INFN, Università di Roma La Sapienza, I-00185 Roma, Italy
- ⁶⁴Universität Rostock, D-18051 Rostock, Germany
- ⁶⁵Rutherford Appleton Laboratory, Chilton, Didcot, Oxon, OX11 0QX, United Kingdom
- ⁶⁶DSM/Dapnia, CEA/Saclay, F-91191 Gif-sur-Yvette, France
- ⁶⁷University of South Carolina, Columbia, South Carolina 29208, USA
- ⁶⁸Stanford Linear Accelerator Center, Stanford, California 94309, USA
- ⁶⁹Stanford University, Stanford, California 94305-4060, USA
- ⁷⁰State University of New York, Albany, New York 12222, USA
- ⁷¹University of Tennessee, Knoxville, Tennessee 37996, USA
- ⁷²University of Texas at Austin, Austin, Texas 78712, USA
- ⁷³University of Texas at Dallas, Richardson, Texas 75083, USA
- ⁷⁴Dipartimento di Fisica Sperimentale and INFN, Università di Torino, I-10125 Torino, Italy
- ⁷⁵Dipartimento di Fisica and INFN, Università di Trieste, I-34127 Trieste, Italy
- ⁷⁶IFIC, Universitat de Valencia-CSIC, E-46071 Valencia, Spain
- ⁷⁷University of Victoria, Victoria, British Columbia, Canada V8W 3P6
- ⁷⁸Department of Physics, University of Warwick, Coventry CV4 7AL, United Kingdom
- ⁷⁹University of Wisconsin, Madison, Wisconsin 53706, USA
- ⁸⁰Yale University, New Haven, Connecticut 06511, USA

*Deceased.

†Also with Università di Perugia, Dipartimento di Fisica, Perugia, Italy.

‡Also with Università della Basilicata, Potenza, Italy.

§Also with Universitat de Barcelona, Facultat de Física, Departament ECM, E-08028 Barcelona, Spain.

||Also with IPPP, Physics Department, Durham University, Durham DH1 3LE, United Kingdom.

(Received 2 August 2007; published 21 December 2007)

We search for decays of a B meson into a neutral D meson and a charged kaon, with the D meson decaying into a charged kaon, a charged pion, and a neutral pion. This final state can be reached through the $b \rightarrow c$ transition $B^- \rightarrow D^0 K^-$ followed by the doubly Cabibbo-suppressed $D^0 \rightarrow K^+ \pi^- \pi^0$, or the $b \rightarrow u$ transition $B^- \rightarrow \bar{D}^0 K^-$ followed by the Cabibbo-favored $\bar{D}^0 \rightarrow K^+ \pi^- \pi^0$. The interference of these two amplitudes is sensitive to the angle γ of the unitarity triangle. We present results based on $226 \times 10^6 e^+ e^- \rightarrow Y(4S) \rightarrow B\bar{B}$ events collected with the *BABAR* detector at SLAC. We find no significant evidence for these decays and we set a limit $R_{\text{ADS}} \equiv \frac{\Gamma([K^+ \pi^- \pi^0]_D K^-) + \Gamma([K^- \pi^+ \pi^0]_D K^+)}{\Gamma([K^+ \pi^- \pi^0]_D K^+) + \Gamma([K^- \pi^+ \pi^0]_D K^-)} < 0.039$ at 95% confidence level, which we translate with a Bayesian approach into $r_B \equiv |A(B^- \rightarrow \bar{D}^0 K^-)/A(B^- \rightarrow D^0 K^-)| < 0.19$ at 95% confidence level.

DOI: 10.1103/PhysRevD.76.111101

PACS numbers: 13.25.Hw, 14.40.Nd

I. INTRODUCTION

Following the discovery of CP violation in B meson decays and the measurement of the angle β of the unitarity triangle [1] associated with the Cabibbo-Kobayashi-Maskawa (CKM) quark mixing matrix, the focus has turned toward the measurements of the other angles α and γ . Following Ref. [2], several methods have been proposed to measure the relative weak phase between the $B^- \rightarrow D^0 K^-$ amplitude, proportional to the CKM matrix element V_{cb} (Fig. 1), and the $B^- \rightarrow \bar{D}^0 K^-$ amplitude, proportional to V_{ub} . This weak phase, which by definition is $\gamma = \arg(-V_{ub}^* V_{ud}/V_{cb}^* V_{cd})$, can be measured from the interference that occurs when the D^0 and the \bar{D}^0 decay to common final states.

As an extension of the method proposed in Ref. [3], we search for $B^- \rightarrow [K^+ \pi^- \pi^0]_D K^-$ [4], where the CKM-favored $B^- \rightarrow D^0 K^-$ decay, followed by the doubly Cabibbo-suppressed $D^0 \rightarrow K^+ \pi^- \pi^0$ decay, interferes with the CKM-suppressed $B^- \rightarrow \bar{D}^0 K^-$ decay, followed by the Cabibbo-favored $\bar{D}^0 \rightarrow K^+ \pi^- \pi^0$ decay.

In order to reduce the systematic uncertainties, we measure ratios of decay rates:

$$R_{\text{ADS}} \equiv \frac{\Gamma([K^+ \pi^- \pi^0]_D K^-) + \Gamma([K^- \pi^+ \pi^0]_D K^+)}{\Gamma([K^+ \pi^- \pi^0]_D K^+) + \Gamma([K^- \pi^+ \pi^0]_D K^-)} = r_B^2 + r_D^2 + 2r_B r_D C \cos \gamma, \quad (1)$$

$$A_{\text{ADS}} \equiv \frac{\Gamma([K^+ \pi^- \pi^0]_D K^-) - \Gamma([K^- \pi^+ \pi^0]_D K^+)}{\Gamma([K^+ \pi^- \pi^0]_D K^-) + \Gamma([K^- \pi^+ \pi^0]_D K^+)} = 2r_B r_D S \sin \gamma / R_{\text{ADS}}, \quad (2)$$

where $r_B \equiv |A(B^- \rightarrow \bar{D}^0 K^-)/A(B^- \rightarrow D^0 K^-)|$, $r_D^2 \equiv \frac{B(D^0 \rightarrow K^+ \pi^- \pi^0)}{B(D^0 \rightarrow K^- \pi^+ \pi^0)}$. The C and S parameters are defined as

$$C = \frac{\int \mathcal{A}_D(\vec{m}) \bar{\mathcal{A}}_D(\vec{m}) \cos(\bar{\delta}(\vec{m}) - \delta(\vec{m}) + \delta_B) d\vec{m}}{\sqrt{\int |\bar{\mathcal{A}}_D(\vec{m})|^2 d\vec{m} \cdot \int |\mathcal{A}_D(\vec{m})|^2 d\vec{m}}}, \quad (3)$$

$$S = \frac{\int \mathcal{A}_D(\vec{m}) \bar{\mathcal{A}}_D(\vec{m}) \sin(\bar{\delta}(\vec{m}) - \delta(\vec{m}) + \delta_B) d\vec{m}}{\sqrt{\int |\bar{\mathcal{A}}_D(\vec{m})|^2 d\vec{m} \cdot \int |\mathcal{A}_D(\vec{m})|^2 d\vec{m}}}, \quad (4)$$

where \vec{m} indicates a point in the Dalitz plane $[m_{K\pi}^2, m_{K\pi^0}^2]$, $[\mathcal{A}_D(\vec{m}), \delta(\vec{m})]$ ($[\bar{\mathcal{A}}_D(\vec{m}), \bar{\delta}(\vec{m})]$) the absolute value, and the strong phase of the D^0 (\bar{D}^0) decay amplitude, and δ_B the strong phase difference between the two interfering B decay amplitudes. Equations (1) and (2) hold when neglecting D -mixing effects, which in the standard model (SM) give negligible corrections to γ [5] and do not affect the r_B measurement.

Determining the angle γ from the measurements of R_{ADS} and A_{ADS} requires extracting the strong phases by means of a Dalitz analysis of the three-body decay of the neutral D meson, for which the available statistics are insufficient. However, with the current statistics we can measure R_{ADS} and constrain r_B by exploiting the fact that in Eq. (1) $|C| \leq 1$. Since the value of r_B is related to the level of interference between the diagrams of Fig. 1, high values of r_B lead to a better sensitivity to γ in any measurement involving $B \rightarrow D^0 K$ decays. Thus, r_B is a key ingredient for the extraction of γ from other measurements [6].

Both the Belle and *BABAR* collaborations have published similar measurements but in a different decay chain, $B \rightarrow DK$ with $D \rightarrow K\pi$ [7]. Unlike those measurements, we can take advantage of the smaller value of r_D , given by $r_D^2 = (0.214 \pm 0.008 \pm 0.008)\%$ [8] in $D \rightarrow K\pi\pi^0$ decays as opposed to $r_D^2 = (0.362 \pm 0.020 \pm 0.027)\%$ [9] in $D \rightarrow K\pi$ decays. This implies that for a given error on R_{ADS} , the sensitivity to r_B is better.

II. EVENT RECONSTRUCTION AND SELECTION

The results presented in this paper are based on $226 \times 10^6 Y(4S) \rightarrow B\bar{B}$ decays collected between 1999 and 2004

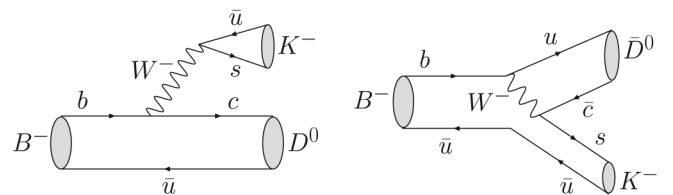


FIG. 1. Feynman diagrams for the CKM-favored $B^- \rightarrow D^0 K^-$ and the CKM- and color-suppressed $B^- \rightarrow \bar{D}^0 K^-$ decays.

with the *BABAR* detector at the PEP-II B factory at SLAC [10]. Approximately 7% of the collected data (15.8 fb^{-1}) have a center-of-mass (CM) energy 40 MeV below the $Y(4S)$ resonance. These “off-resonance” data are used to study backgrounds from continuum events, $e^+e^- \rightarrow q\bar{q}$ ($q = u, d, s, \text{ or } c$). The *BABAR* detector is described elsewhere [11]. Charged-particle tracking is provided by a five-layer silicon vertex tracker (SVT) and a 40-layer drift chamber (DCH). In addition to providing precise position information for tracking, the SVT and DCH also measure the specific ionization (dE/dx), which is used for particle identification of low-momentum charged particles. At higher momenta ($p > 0.7 \text{ GeV}/c$) pions and kaons are identified by Cherenkov radiation detected in a ring-imaging device (DIRC). The position and energy of photons are measured with an electromagnetic calorimeter (EMC) consisting of 6580 thallium-doped CsI crystals. These systems are mounted inside a 1.5T solenoidal superconducting magnet.

The event selection was developed from studies of off-resonance data and $B\bar{B}$ and continuum events simulated with Monte Carlo (MC) techniques. A large on-resonance data sample of $B^- \rightarrow D^0\pi^-$, $D^0 \rightarrow K^-\pi^+\pi^0$ events was used to validate several aspects of the simulation and analysis procedure. We refer to this mode as $B \rightarrow D\pi$.

Both kaon candidates are required to satisfy kaon identification criteria, which are based on the specific ionization loss measured in the tracking devices and on the Cherenkov angles measured in the DIRC and are typically 85% efficient, depending on momentum and polar angle. Misidentification rates are at the 2% level. The π^0 candidates are reconstructed as pairs of photon candidates in the EMC, each with energy larger than 70 MeV and a lateral shower profile consistent with an electromagnetic deposit. These pairs must have a total energy greater than 200 MeV and $118 < m_{\gamma\gamma} < 145 \text{ MeV}/c^2$. To account for the correlation between the tails in the distribution of the $K\pi\pi^0$ invariant mass and the π^0 candidate mass, we require the difference between the two measured masses to be within $32.5 \text{ MeV}/c^2$ of the expected value of $m_{D^0} - m_{\pi^0} = 1729.5 \text{ MeV}/c^2$ [12], retaining 90% of the signal. The remaining background from other $B^\pm \rightarrow [h_1h_2\pi^0]_D h_3^\pm$ [4] modes is reduced by removing events where the invariant mass of any $h_1h_2\pi^0$ candidate, with any particle-type assignment other than the signal hypothesis, is consistent with the D^0 meson mass, retaining 92% of the signal.

After these requirements, the background is mostly due to $D^0\bar{D}^0$ pair production in $e^+e^- \rightarrow c\bar{c}$ events, with $\bar{D}^0 \rightarrow K^+\pi^-\pi^0$ and $D \rightarrow K^-$. To discriminate between the signal and this dominant background we use a neural network (NNet) with six quantities that distinguish continuum and $B\bar{B}$ events: $L_0 = \sum_i p_i$ and $L_2 = \sum_i p_i \cos^2 \theta_i$, both calculated in the CM frame, where p_i is the momentum of particle i , θ_i is its angle relative to the thrust axis of the B candidate, and the sum runs over all tracks and clusters

not used to reconstruct the B candidate; the angle in the CM frame between the thrust axes of the B candidate and of the detected remainder of the event; the polar angle of the B candidate in the CM frame; the distance of closest approach between the track of the kaon candidate from the B and the trajectory of the reconstructed D meson (this is consistent with zero for signal events, but can be larger in $c\bar{c}$ events); the distance along the beams between the reconstructed vertex of the B candidate and the vertex of the other tracks in the event, this is consistent with zero for continuum events, but is sensitive to the B lifetime for signal events.

The NNet is trained with simulated continuum and signal events. We find agreement between the distributions of all six variables in simulation, off-resonance data, and $B \rightarrow D\pi$ events. We apply a loose preselection on the NNet ($0.4 < \text{NNet} < 1.0$) with a 90% efficiency for signal and a 68% rejection power for continuum, and then use the NNet itself in the likelihood fit described below to fully exploit its discriminating power.

A B -meson candidate is characterized by the energy-substituted mass $m_{\text{ES}} \equiv \sqrt{(\frac{s}{2} + \vec{p}_0 \cdot \vec{p}_B)^2 / E_0^2 - p_B^2}$ and energy difference $\Delta E \equiv E_B^* - \frac{\sqrt{s}}{2}$, where E and p are energy and momentum, the asterisk denotes the CM frame, the subscripts 0 and B refer to the initial e^+e^- state and B candidate, respectively, and s is the square of the CM energy. For signal events, m_{ES} is centered around the B mass with a resolution of about $2.5 \text{ MeV}/c^2$, and ΔE is centered at zero with a resolution of 17 MeV.

Considering both the case where the two kaons have the same and the opposite charge (referred to as “same-sign” and “opposite-sign” samples, respectively), 28 621 events survive the selection described above and the loose requirements $|\Delta E| < 100 \text{ MeV}$ and $m_{\text{ES}} > 5.2 \text{ GeV}/c^2$. While the dominant background comes from continuum events, there is still a nonnegligible contribution from $Y(4S) \rightarrow B\bar{B}$ events (denoted “ $B\bar{B}$ ” in the following). We consider separately the $B \rightarrow D\pi$ background, since it differs from the signal only in the ΔE distribution. For this decay mode the opposite-sign $B^- \rightarrow \bar{D}^0\pi^-$ amplitude is suppressed by a factor $\approx r_B \lambda^2$, where $\lambda \approx 0.22$ is the sine of the Cabibbo angle. Therefore we expect to find a non-negligible $B \rightarrow D\pi$ background only in the same-sign sample.

III. LIKELIHOOD FIT AND RESULTS

The signal and background yields are extracted by maximizing the extended likelihood $\mathcal{L} = e^{-N'} \prod_{i=1}^N \mathcal{L}_i(\vec{x}_i) / N!$. Here $N' = N_{DK} + N_{\text{cont}} + N_{BB} + N_{D\pi}$ is the sum of the yields of the signal and the three background contributions (including both the same-sign and the opposite-sign components), $\vec{x} = \{\text{NNet}, \Delta E, m_{\text{ES}}\}$, N is the number of events in the selected sample, and the likelihood of the individual events (\mathcal{L}_i) is

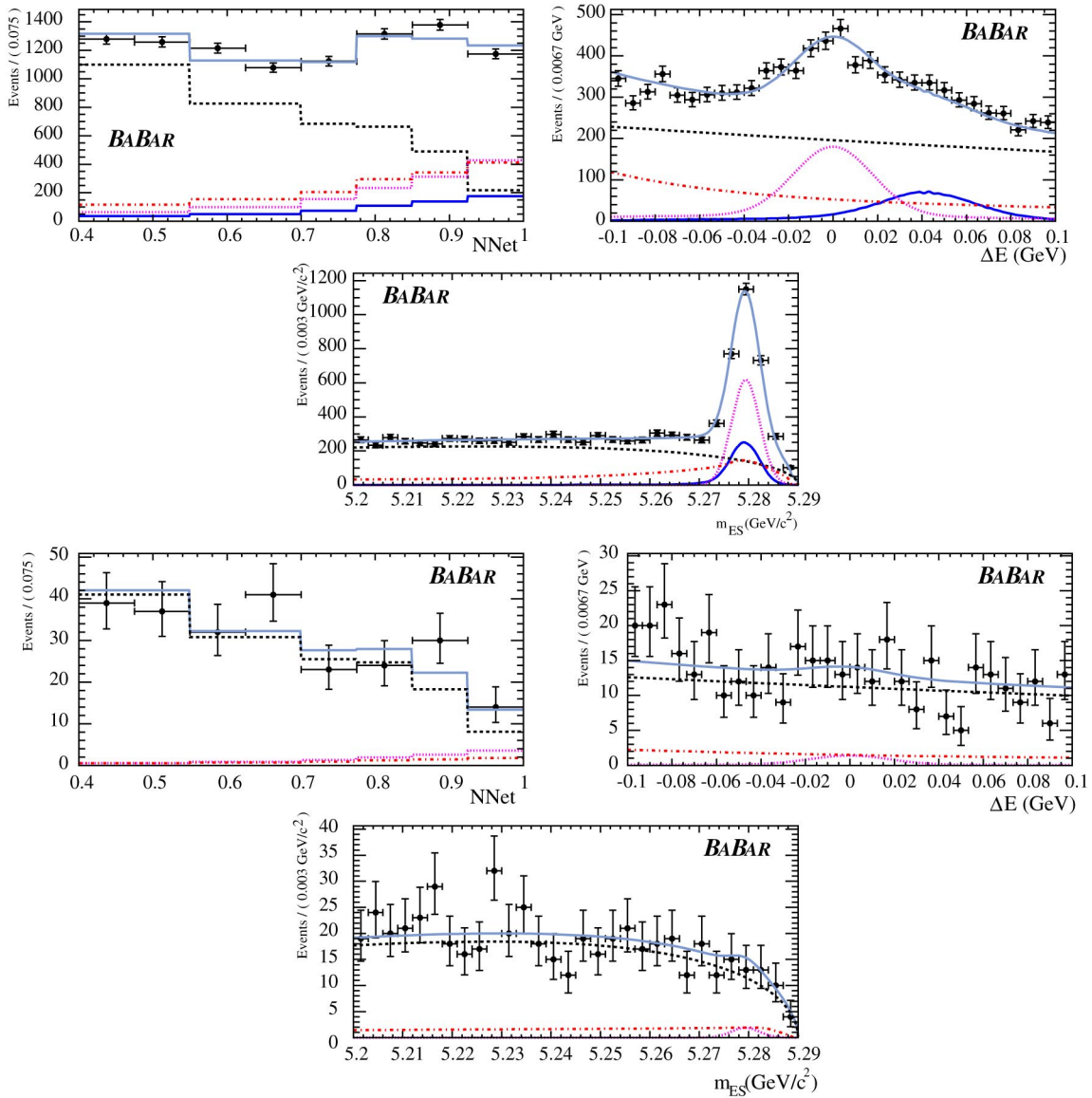


FIG. 2 (color online). Likelihood fit projections of the NNet, ΔE , and m_{ES} distributions separately for the same (top) and opposite (bottom) sign samples. To visually enhance the signal, the distributions for the latter sample are shown after cuts, with a 67% signal efficiency, on the ratios between the signal and the total likelihood of all the variables other than the one shown. The points with error bars represent the data, while the dashed, dashed-dotted, and solid lines represent the contributions from continuum, $B\bar{B}$, and $D\pi$ backgrounds, respectively. The dotted line represents the signal contribution, visible only in the same-sign sample.

defined as

$$\begin{aligned} \mathcal{L}_i(\vec{x}_i) = & \frac{N_{DK}}{1 + R_{ADS}} f_{DK}^{RS}(\vec{x}_i) + \frac{N_{\text{cont}}}{1 + R_{\text{cont}}} f_{\text{cont}}^{RS}(\vec{x}_i) \\ & + \frac{N_{BB}}{1 + R_{BB}} f_{BB}^{RS}(\vec{x}_i) + N_{D\pi} f_{D\pi}(\vec{x}_i) \end{aligned} \quad (5)$$

for same-sign events and

$$\begin{aligned} \mathcal{L}_i(\vec{x}_i) = & \frac{N_{DK} R_{ADS}}{1 + R_{ADS}} f_{DK}^{WS}(\vec{x}_i) + \frac{N_{\text{cont}} R_{\text{cont}}}{1 + R_{\text{cont}}} f_{\text{cont}}^{WS}(\vec{x}_i) \\ & + \frac{N_{BB} R_{BB}}{1 + R_{BB}} f_{BB}^{WS}(\vec{x}_i) \end{aligned} \quad (6)$$

for opposite-sign events. In these equations we have defined R parameters for the backgrounds analogous to those for the signal, defined in Eq. (1). The individual probability density functions (PDFs) f are derived from MC and are built as the product of one-dimensional distributions of the three variables. The only exception is the m_{ES} and ΔE PDF for the $D\pi$ background, where we use a two-dimensional nonparametric distribution [13] due to a nonnegligible correlation between these two variables. The NNet distributions are all modeled with a histogram with eight bins between 0.4 and 1. The m_{ES} distributions are modeled with a Gaussian in the case of the signal, a threshold function

[14] in the case of the continuum background, and the sum of a threshold function and a Gaussian function with an exponential tail in the case of the $B\bar{B}$ background. Finally, the ΔE distributions are parametrized with the sum of two Gaussians in the case of the signal, an exponential in the case of the continuum background, and a sum of two exponentials in the case of the $B\bar{B}$ background. For m_{ES} and ΔE of the $B\bar{B}$ and continuum background, we use different parameters for same-sign and opposite-sign sample.

We perform the fit by floating the four total yields (N_{DK} , N_{cont} , N_{BB} , and $N_{D\pi}$), the three R variables and the shape parameters of the threshold function used to parametrize the m_{ES} distribution for the same- and opposite-sign continuum background separately. Figure 2 shows the distributions of the three variables in the selected sample, with the likelihood projections overlaid. The fit yields $R_{ADS} = 0.013_{-0.004}^{+0.010}$, $N_{DK} = (14.7 \pm 0.6) \times 10^2$, $N_{cont} = (239.3 \pm 2.1) \times 10^2$, $N_{BB} = (25.5 \pm 1.6) \times 10^2$, $N_{D\pi} = (6.7 \pm 0.4) \times 10^2$, $R_{cont} = 3.05 \pm 0.07$, $R_{BB} = 0.42 \pm 0.07$.

Equation (5) assumes equal efficiencies for the same- and opposite-sign signal samples, regardless of the difference in the Dalitz structure. This has been demonstrated to be true in MC within a relative statistical error of 4%. We then consider this as a systematic error on R_{ADS} . We also repeat the fit by varying the PDF parameters obtained from MC within their statistical errors and by estimating $f_{cont}^{RS/WS}$ on off-resonance data and $f_{DK}^{RS/WS}$ on exclusively reconstructed $D\pi$ events. To account for the observed variations, we assign a 0.0076 systematic error on R_{ADS} . The uncertainty due to B decays with distributions similar to the signal, in particular $B \rightarrow D^{(*)}\pi$, D^*K , $D^{(*)}K^*$, and $KK\pi\pi^0$, is estimated by varying their branching fractions within their known errors and found to be $6 \cdot 10^{-5}$ on R_{ADS} , and therefore negligible. The quality of the simulation of B decays to final states with charm mesons that might mimic the signal has been checked by comparing data and MC samples in the sidebands of the ΔE distribution where these decays dominate. Similarly, we searched the sidebands of the $m_{D^0} - m_{\pi^0}$ distribution for background from charmless B decays and found no evidence of it.

Following a Bayesian approach, we extract r_B by defining the posterior distribution

$$\mathcal{L}(r_B) = \frac{\int p(r_B, r_D, \xi) \mathcal{L}(R_{ADS}(r_B, r_D, \xi)) dr_D d\xi}{\int p(r_B, r_D, \xi) \mathcal{L}(R_{ADS}(r_B, r_D, \xi)) dr_D d\xi dr_B}, \quad (7)$$

where $\xi = C \cos \gamma$, $R_{ADS}(r_B, r_D, \xi)$ is given in Eq. (1), and $p(r_B, r_D, \xi)$ is the prior distribution for these three quantities. They are considered uncorrelated, with ξ and r_B uniformly distributed in the range of $[-1, 1]$ and $[0, 1]$, respectively. The prior distribution for r_D is a Gaussian

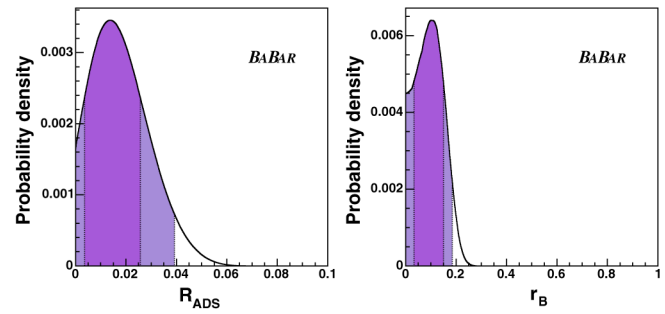


FIG. 3 (color online). Likelihood function for R_{ADS} (left) and r_B (right). The latter is obtained in a Bayesian approach, assuming flat prior distributions for r_B and $\xi = C \cos \gamma$. The 68% and 95% regions are shown in dark and light shading, respectively.

consistent with $r_D^2 = (0.214 \pm 0.008 \pm 0.008)\%$ [8]. The likelihood $\mathcal{L}(R_{ADS})$ is obtained by convolving the likelihood returned by the fit with a Gaussian of width 0.0076, equivalent to the systematic uncertainty.

Figure 3 shows $\mathcal{L}(R_{ADS})$ and $\mathcal{L}(r_B)$. We set a 95% confidence level (C.L.) limit by integrating the likelihood, starting from $R_{ADS} = 0$ ($r_B = 0$), thus excluding unphysical values, and we define the 68% C.L. region, for each variable $r = R_{ADS}$ or r_B , as the interval where $\mathcal{L}(r) > \mathcal{L}_{min}$ and $68\% = \int_{\mathcal{L}(r) > \mathcal{L}_{min}} \mathcal{L}(r) dr$.

IV. CONCLUSIONS

In summary, we measure the ratio of the rate for the $B^\pm \rightarrow [K^\mp \pi^\pm \pi^0]_D K^\pm$ decay to the favored decay $B^\pm \rightarrow [K^\pm \pi^\mp \pi^0]_D K^\pm$ to be $R_{ADS} = 0.013_{-0.010}^{+0.012}$. While this result is consistent with and similar in sensitivity to the completely independent previously published results [7], it is obtained using a different D decay mode. Because the measurement is not statistically significant, we set a 95% C.L. limit $R_{ADS} < 0.039$. We use this information to infer the ratio between the rates of the $B^- \rightarrow \bar{D}^0 K^-$ and $B^- \rightarrow D^0 K^-$ decays to be $r_B = 0.091 \pm 0.059$ and consequently set a limit $r_B < 0.19$ at 95% C.L.

ACKNOWLEDGMENTS

We are grateful for the excellent luminosity and machine conditions provided by our PEP-II colleagues, and for the substantial dedicated effort from the computing organizations that support BABAR. The collaborating institutions wish to thank SLAC for its support and kind hospitality. This work is supported by DOE and NSF (USA), NSERC (Canada), IHEP (China), CEA and CNRS-IN2P3 (France), BMBF and DFG (Germany), INFN (Italy), FOM (The Netherlands), NFR (Norway), MIST (Russia), MEC (Spain), and PPARC (United Kingdom). Individuals have received support from the Marie Curie EIF (European Union) and the A. P. Sloan Foundation.

B. AUBERT *et al.*PHYSICAL REVIEW D **76**, 111101(R) (2007)

- [1] B. Aubert *et al.* (BABAR Collaboration), Phys. Rev. Lett. **89**, 201802 (2002); K. Abe *et al.* (Belle Collaboration), Phys. Rev. D **66**, 071102 (2002).
- [2] M. Gronau and D. Wyler, Phys. Lett. B **265**, 172 (1991); M. Gronau and D. London, Phys. Lett. B **253**, 483 (1991).
- [3] D. Atwood, I. Dunietz, and A. Soni, Phys. Rev. Lett. **78**, 3257 (1997); Phys. Rev. D **63**, 036005 (2001).
- [4] Charge conjugation is implied throughout the paper. Also, we use the notation $B^- \rightarrow [h_1^+ h_2^- \pi^0]_D h_3^-$ (with $h_i = \pi$ or K) for the decay chains $B^- \rightarrow \tilde{D}^0 h_3^-$, where \tilde{D}^0 is either a D^0 or a \bar{D}^0 and $\tilde{D}^0 \rightarrow h_1^+ h_2^- \pi^0$. We also refer to h_3 as the π or K from the B .
- [5] Y. Grossman, A. Soffer, and J. Zupan, Phys. Rev. D **72**, 031501 (2005).
- [6] B. Aubert *et al.* (BABAR Collaboration), Phys. Rev. Lett. **95**, 121802 (2005).
- [7] B. Aubert *et al.* (BABAR Collaboration), Phys. Rev. D **72**, 032004 (2005); M. Saigo *et al.* (Belle Collaboration), Phys. Rev. Lett. **94**, 091601 (2005).
- [8] B. Aubert *et al.* (BABAR Collaboration), Phys. Rev. Lett. **97**, 221803 (2006).
- [9] B. Aubert *et al.* (BABAR Collaboration), Phys. Rev. Lett. **91**, 171801 (2003).
- [10] PEP-II Conceptual Design Report, SLAC-0418, 1993.
- [11] B. Aubert *et al.* (BABAR Collaboration), Nucl. Instrum. Methods Phys. Res., Sect. A **479**, 1 (2002).
- [12] S. Eidelman *et al.* (Particle Data Group), Phys. Lett. B **592**, 031501 (2004) and 2005 partial update for the 2006 edition.
- [13] K. Cranmer, Comput. Phys. Commun. **136**, 198 (2001).
- [14] H. Albrecht *et al.* (ARGUS Collaboration), Z. Phys. C **48**, 543 (1990).